The Ferromagnetic Chain System *catena*-(μ-CrO_4-*O,O′*)[Ni^{II}(cyclam)]·$2H_2O$

Hiroki Oshio,*,† Hiroshi Okamoto,‡ Toshihiko Kikuchi,† and Tasuku Ito†

Department of Chemistry, Graduate School of Science, Tohoku University, Aoba-ku, Sendai 980-77, Japan, and Research Institute for Scientific Measurements, Tohoku University, Aoba-ku, Sendai 980-77, Japan

Received February 20, 1997

Introduction

There has been increasing interest in low-dimensional magnetic systems which show peculiar quantum effects. One-dimensional Ni^{II} systems with antiferromagnetic intrachain interactions have been extensively studied from this point of view.[1] Some experimental results[2] have proven the Haldane prediction;[3] that is, there is a singlet−triplet energy gap for the integer spin system. In contrast, only a few one-dimensional Ni^{II} systems with intrachain ferromagnetic interactions have been reported; for example, double end-on azido-bridged Ni^{II} complexes showed intrachain ferromagnetic interactions ($J = 11.9-21.7$ cm^{-1}; $H = -2J\sum S_i \cdot S_j$)[4] and a *trans*-cyanato *catena* Ni^{II} complex showed weak intrachain ferromagnetic interactions ($J = 2.3$ cm^{-1}; $H = -2J\sum S_i \cdot S_{i+1}$).[5] On the other hand, $[CrO_4]^{2-}$ units have been known to act as bridging ligands, and some $[CrO_4]^{2-}$ bridged metal complexes have been magnetically and structurally characterized.[6] A dinuclear Cu^{II} complex, [{Cu^{II}(acpa)}$_2$(μ-CrO_4)] (acpa = tridentate Schiff base ligand), showed ferromagnetic interactions ($2J = 14.6(1)$ cm^{-1}; $H = -2JS_1 \cdot S_2$),[7] while antiferromagnetic interactions are operative in other metal complexes.[8] Here we report the structure and magnetic and optical properties of a ferromagnetic chain system *catena*-(μ-CrO_4-*O,O′*)[Ni^{II}(cyclam)]·$2H_2O$ (**1**) (cyclam = 1,4,8,11-tetraazacyclotetradecane).

Experimental Section

Preparation of *catena*-(μ-CrO_4-*O,O′*)[Ni^{II}(cyclam)]·$2H_2O$ (1). A solution of K_2CrO_4 (194 mg, 1 mmol) and triethylamine (101 mg, 1 mmol) in water (10 mL) was added to a solution of the [Ni^{II}(cyclam)]-$(ClO_4)_2$ (458 mg, 1 mmol) in water (5 mL). After the solution was left to stand overnight, dark red tablets of **1** were filtered out and one of them was subjected to the X-ray structural analysis. Anal. Calcd for $C_{10}H_{28}CrN_4NiO_6$: C, 29.22; H, 6.87; N,13.63. Found: C, 28.98; H, 6.42; N, 13.38.

Physical Measurements. Magnetic susceptibility data were collected in the temperature range 2.0−300 K in an applied field of 1 T with the use of a Quantum Design Model MPMS SQUID magnetometer. Pascal's constants were used to determinate the constituent atom diamagnetism.[9] Polarized reflection spectra was measured by using a halogen−tungsten incandescent lamp. Light from the lamp was focused by a concave mirror on the entrance slit of a 25 cm grating monochromator (JASCO GD25). The monochromatic light from the exit slit was passed through a polarizer and was focused on the specific surface of a single crystal sample by using an optical microscope. Reflected light from the sample was focused by a concave mirror on the detector (A PbS cell or a photomultiplier tube).

X-ray Crystallography. Table 1 lists the crystallographic data. Crystal of **1** with dimensions of $0.3 \times 0.4 \times 0.5$ mm^3 was used for

Table 1. Crystal and Refinement Data for *catena*-(μ-CrO_4-*O,O′*)[Ni(cyclam)]·$2H_2O$

formula	$C_{10}H_{28}CrN_4NiO_6$
fw	411.05
temp (°C)	−60
space group	$P\bar{1}$ (No. 2)
a (Å)	9.156(2)
b (Å)	12.168(2)
c (Å)	9.027(3)
α (deg)	92.86(2)
β (deg)	117.74(2)
γ (deg)	105.06(2)
V (Å^3)	842.2(2)
Z	2
ρ_{calc} (g cm^{-3})	1.621
ρ_{obsd} (g cm^{-3})	1.64
λ(Mo Kα) (Å)	0.710 73
μ(Mo Kα) (cm^{-1})	18.2
R[a]	0.027
R_w[b]	0.036

[a] $R = \sum(|F_o| - |F_c|)/\sum|F_o|$. [b] $R_w = [\sum w(|F_o| - |F_c|)^2/\sum w|F_o|^2]^{1/2}$. $w = (\sigma_c^2 + (0.02|F_o|)^2)^{-1}$.

Table 2. Fractional Coordinates and Equivalent Isotropic Displacement Parameters (Å^2) of Non-Hydrogen Atoms of *catena*-(μ-CrO_4-*O,O′*)[Ni(cyclam)]·$2H_2O$

	x/a	y/b	z/c	U[a]
Ni(1)	0	0	1	0.0128(1)
Ni(2)	1/2	1/2	1	0.0146(1)
Cr	0.18907(4)	0.29116(2)	1.05547(4)	0.0152(1)
O(1)	0.1162(2)	0.1556(1)	0.9515(2)	0.0201(6)
O(2)	0.2702(2)	0.3808(1)	0.9620(2)	0.0220(6)
O(3)	0.0267(2)	0.3243(1)	1.0602(2)	0.0294(7)
O(4)	0.3429(2)	0.3004(1)	1.2511(2)	0.0276(6)
O(5)	−0.1616(3)	0.4292(2)	0.7908(3)	0.0380(8)
O(6)	0.6419(4)	0.2454(2)	0.4946(3)	0.066(1)
N(1)	−0.1534(2)	−0.0592(1)	0.7385(2)	0.0171(7)
N(2)	0.1970(2)	−0.0638(1)	1.0213(2)	0.0173(7)
N(3)	0.5335(3)	0.3766(2)	0.8645(3)	0.0283(9)
N(4)	0.3543(2)	0.5597(2)	0.7876(3)	0.0260(8)
C(1)	−0.2830(3)	0.0031(2)	0.6805(3)	0.0245(9)
C(2)	−0.0573(3)	−0.0485(2)	0.6438(3)	0.0227(9)
C(3)	0.0780(3)	−0.1113(2)	0.7082(3)	0.0252(9)
C(4)	0.2382(3)	−0.0520(2)	0.8824(3)	0.0223(9)
C(5)	0.3474(3)	−0.0067(2)	1.1924(3)	0.0249(9)
C(6)	0.2297(3)	0.4720(3)	0.6310(3)	0.041(1)
C(7)	0.3189(4)	0.4009(3)	0.5819(4)	0.051(1)
C(8)	0.3794(4)	0.3165(2)	0.6949(4)	0.045(1)
C(9)	0.5952(4)	0.2980(2)	0.9807(4)	0.042(1)
C(10)	0.2742(4)	0.6319(2)	0.8429(4)	0.041(1)

[a] Equivalent isotropic *U* defined as one-third of the trace of the orthogonalized $\mathbf{U}_{ij}$ tensor.

† Department of Chemistry.
‡ Research Institute for Scientific Measurements.

(1) (a) Ribas, J.; Monfort, M.; Diaz, C.; Bastos, C.; Mer, C.; Solans, X. *Inorg. Chem*. **1995**, *34*, 4986. (b) Escuer, A.; Vicente, R.; Ribas, J.; Fallkah, M. S. E.; Solans, X.; Bardía, M. F. *Inorg. Chem*. **1994**, *33*, 1842.
(2) (a) Meyer, A.; Gleizes, A.; Girerd, J.; Verdaguer, M.; Kahn, O. *Inorg. Chem*. **1982**, *21*, 1729. (b) Yamashita, M.; Inoue, K.; Ohishi, T.; Takeuchi, T.; Yoshida, T.; Mori, W. *Mol. Crysl. Liq. Cryst*. **1995**, *274*, 25.
(3) (a) Haldane, F. D. M. *Phys. Lett*. **1983**, *93A*, 46. (a) Haldane, F. D. M. *Phys. Rev. Lett.* **1983**, *50*, 1153.
(4) Ribas, J.; Monfort,.M.; Diaz, C.; Bastos, C.; Solans, X. *Inorg. Chem*. **1994**, *33*, 489.
(5) Escuer, A.; Vicente, R.; El Fallah, M. S.; Solans, X.; Baría, M. F. *J. Chem. Soc., Dalton Trans*. **1996**, 1013.
(6) (a) Harel, M.; Knobler, C.; McCullough, T. D. *Inorg. Chem*. **1969**, *8*, 11. (b) Gatehouse, B. M.; Guddat, L. W. *Acta Crystallogr., Sect. C: Cryst. Struct. Commun*. **1987**, *C43*, 1445. (c) Bensch, W.; Seferiadis, N.; Oswald, H. R. *Inorg. Chim. Acta* **1987**, *126*, 113.
(7) Oshio, H.; Kikuchi, T.; Ito, T. *Inorg. Chem*. **1996**, *35*, 4938−4941.
(8) Chaudhuri, P.; Winter, M.; Wieghardt, K.; Gehring, S.; Haase, W.; Nuber, B.; Weiss, J. *Inorg. Chem*. **1988**, *27*, 1564.
(9) Boudreaux, E. A., Mulay, L. N., Eds. *Theory and Application of Molecular Paramagnetism*; Wiley and Sons, Inc.: New York, 1976.

S0020-1669(97)00180-8 CCC: $14.00

Table 3. Selected Bond Lengths (Å) and Angles (deg) of *catena*-(μ-CrO_4-*O*,*O*′)[Ni(cyclam)]·$2H_2O$

Ni(1)−O(1)	2.092(1)	Ni(1)−N(1)	2.069(2)
Ni(1)−N(2)	2.076(2)	Ni(2)−O(2)	2.083(2)
Ni(2)−N(3)	2.062(3)	Ni(2)−N(4)	2.061(2)
Cr−O(1)	1.655(1)	Cr−O(2)	1.646(2)
Cr−O(3)	1.657(2)	Cr−O(4)	1.642(1)
Ni(1)−Cr	3.4100(6)	Ni(1)−Ni(2)	6.5954(9)
Ni(2)−Cr	3.5366(6)		
O(1)−Ni(1)−N(1)	87.94(6)	O(1)−Ni(1)−N(2)	90.91(7)
O(1)−Ni(1)−N(1)	92.06(6)	O(1)−Ni(1)−N(2)	89.09(7)
N(1)−Ni(1)−N(2)	94.68(8)	O(2)−Ni(2)−N(3)	90.21(8)
O(2)−Ni(2)−N(4)	88.83(7)	O(2)−Ni(2)−N(3)	89.79(8)
O(2)−Ni(2)−N(4)	91.17(7)	N3−Ni(2)−N4	94.29(9)
O(1)−Cr−O(2)	110.45(9)	O(1)−Cr−O(3)	109.06(8)
O(1)−Cr−O(4)	108.12(8)	O(2)−Cr−O(3)	110.19(9)
O(2)−Cr−O(4)	109.25(8)	O(3)−Cr−O(4)	109.7(1)
Ni(1)−O(1)−Cr	130.7(1)	Ni(2)−O(2)−Cr	142.75(8)

data collection. Diffraction data at −60 °C were collected on Rigaku AFC7S diffractometer equipped with graphite monochromatized Mo Kα (λ = 0.710 73 Å) radiation. Three standard reflections were measured every 200 data collections and revealed no fluctuation in intensities. The lattice constants were optimized from a least-squares refinement of settings of 25 carefully centered Bragg reflections in the range 25° < 2θ < 30°. Data were corrected for Lorentz and polarization. An empirical absorption correction by using the ψ scan method was applied which resulted in transmission factors ranging from 0.99 to 1.06. The maximum 2θ value for the data collection was 55°. The numbers of measured and unique reflections were 4102 and 3858, respectively. The structure was solved by a conventional heavy atom method and refined by the full-matrix least-squares method with anisotropic thermal parameters for non-hydrogen atoms and isotropic ones for hydrogen atoms. Final R and R_w values are 0.027 and 0.036, respectively, for 3444 unique reflections with $I_o > 3\sigma(I_o)$ and 314 parameters. The final Fourier difference synthesis showed a maximum and minimum of +0.49 and −0.84 e Å^3, respectively. All calculations were performed by using Xtal 3.2.[10] Final atomic parameters and equivalent isotropic thermal parameters for non-hydrogen atoms are listed in Table 2.

Results and Discussion

The reaction of $[Ni^{II}(cyclam)](PF_6)_2$ with K_2CrO_4 in water gave dark red tablets of **1**. Complex **1** crystallizes in the triclinic space group $P\bar{1}$. Selected bond lengths and angles were listed in Table 3. In **1**, the crystal consists of a $[CrO_4]^{2-}$ anion, water molecules, and two kinds of crystallographically independent $[Ni(cyclam)]^{2+}$ cations located on the center of inversion. The coordination geometry about each Ni^{II} ion is octahedral, where the equatorial coordination sites of the Ni^{II} ions are occupied by four nitrogen atoms from cyclam (Ni−N = 2.061(2)−2.076(2) Å) and the axial sites are completed by two oxygen atoms from $[CrO_4]^{2-}$ anion (Ni−O = 2.083(2)−2.092(1) Å). $[CrO_4]^{2-}$ anions bridge the Ni^{II} ions and form a one-dimensional structure (Figure 1) with the Ni−Cr separation of 3.4100(6)−3.5366(6) Å.

The magnetic susceptibility data for **1** are shown in the form of $\chi_m T$ vs T plots (Figure 2). $\chi_m T$ values increase as the temperature is lowered to 9 K, which is indicative of a ferromagnetic interaction. In **1**, the Ni−Ni separation within the chain is 6.5954(9) Å, while the closest Ni−Ni separation between the chain is 8.512(1) Å. The observed ferromagnetic interaction is, therefore, due to the intrachain interaction. Fisher's model[11] for the classical-spin chain system ($S = 1$ and $H_{chain} = -J\sum S_i \cdot S_{i+1}$) was applied to the analysis of the magnetic

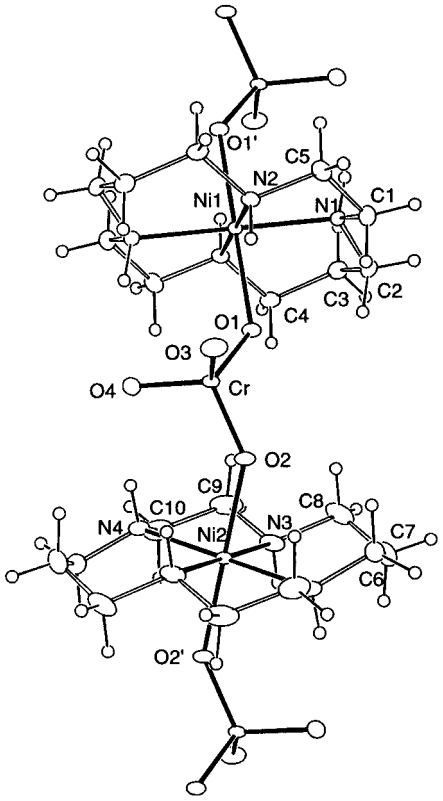

Figure 1. One-dimensional structure of **1** showing 30% thermal ellipsoids.

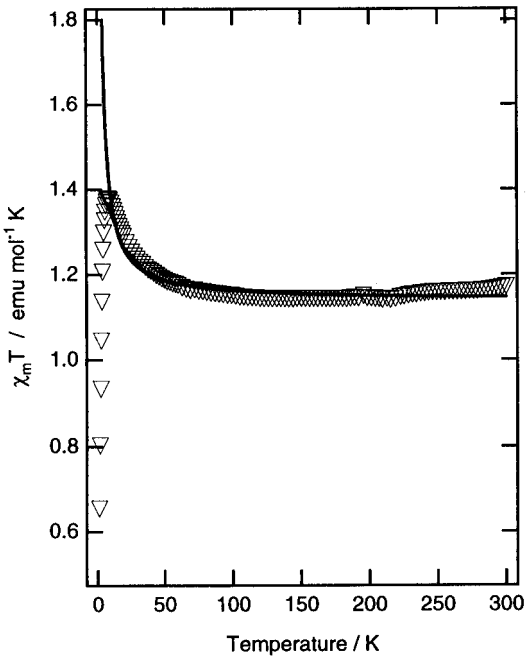

Figure 2. Temperature dependence of $\chi_m T$ values for **1**. The solid line corresponds to the best-fitted curves by using the parameters described in the text.

data. The magnetic susceptibility χ_m can be expressed as

$$\chi_m = \frac{Ng^2\beta^2 S(S+1)}{3kT}\frac{1+u}{1-u}$$

$$u = \coth\left[\frac{JS(S+1)}{kT}\right] - \left[\frac{kT}{JS(S+1)}\right]$$

where the symbols have their usual meaning. The least-squares

(10) Hall, S. R.; Sterwart J. M. Xtal 3.2 Manual, University of Western Australia and Maryland.
(11) Fisher, M. E. *Am. J. Phys.* **1964**, *32*, 343.

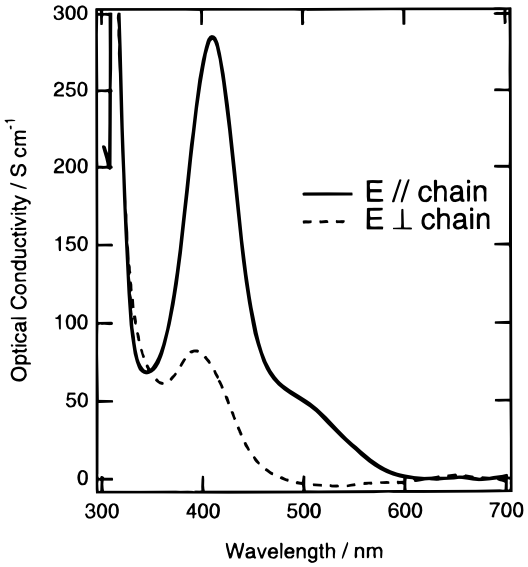

Figure 3. Optical conductivity spectra of **1** for the single crystal with *E* parallel to the chain (—) and *E* perpendicular to the chain (- - -).

fitting of the observed data above 9 K led to $J = +0.6(1)$ cm^{-1} and $g = 2.13(1)$. In this fitting, the contribution of the zero field splitting of the Ni^{II} ion was ignored because of the octahedral coordination geometry of the Ni^{II} ions. The sudden decrease of $\chi_m T$ values below 9 K might be due to an antiferromagnetic interchain interaction.

Optical conductivity spectra of **1**, which were obtained by the Kramers−Kronig transformation from the polarized reflectivity spectra for the single crystal, are depicted in Figure 3. When the electric vector *E* is parallel to the chain ($E_{\parallel}$ chain), a strong absorption band (410 nm) with a shoulder (510 nm) was observed, where the band at 410 nm was assigned to the LMCT(O→Cr) band.[12] When *E* is perpendicular to the chain ($E_{\perp}$ chain), the shoulder band disappeared. UV−vis spectra of [Ni(cyclam)](PF_6) and K_2CrO_4 in water showed a d−d band at 460 nm ($\epsilon = 60$ M^{-1} cm^{-1}) and a LMCT band at 372 nm ($\epsilon = 1900$ M^{-1} cm^{-1}), respectively. The intensity ratio ($I_{shoulder}/I_{LMCT(O\rightarrow Cr)} = 0.20$) of the shoulder band to the LMCT(O→Cr) band in **1** is much bigger than that for which would be expected for the d−d band of the Ni^{II} ion ($I_{Ni(d-d)}/I_{LMCT(O\rightarrow Cr)} = 0.03$). The absorption band at 510 nm can be assigned to the LMCT band from the coordinated oxygen atom to the Ni^{II} ion. Due to the LMCT(O→Ni) interaction, the spin on the d_{z^2} orbital is considered to delocalize onto the coordinated oxygen atom of $[CrO_4]^{2-}$ anion.

(12) (a) Duiker, J. C.; Ballhausen, C. J. *Theoret. Chim. Acta* **1968**, *12*, 325. (b) Johnson, L. W.; McGlynn, S. P. *Chem. Phys. Lett.* **1970**, *7*, 618. (c) Miller, R. M.; Tinti, D. S.; Case. D. A. *Inorg. Chem.* **1989**, *28*, 2738.

Scheme 1

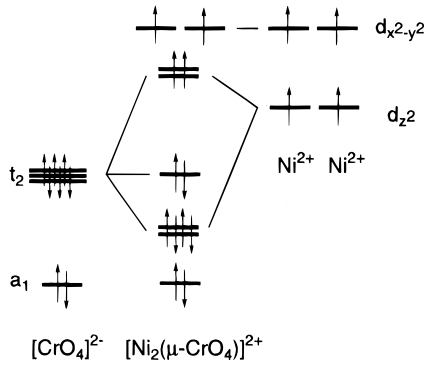

Propagation of the ferromagnetic interaction in **1** can be understood by the orbital topology of the frontier orbitals. Under T_d symmetry $[CrO_4]^{2-}$ ion has triply degenerate HOMOs (highest occupied molecular orbital), being combinations of t_2-type chromium d and coordinated oxygen p orbitals. When the $[CrO_4]^{2-}$ anion bridges Ni^{II} ions from their axial sites, each having two spins on d_{z^2} and $d_{x^2-y^2}$ orbitals, the d_{z^2} of the Ni^{II} ions and two of the triply degenerate orbitals of the $[CrO_4]^{2-}$ fragment form two sets of σ-type bonding and antibonding orbitals. The d_{z^2} orbitals of the Ni^{II} ions and the oxygen p orbitals interact to mix through the LMCT(O→Ni) interaction. The two unpaired electrons from the d_{z^2} orbitals occupy the antibonding orbitals, while the $d_{x^2-y^2}$ and remainder of the $[CrO_4]^{2-}$ orbitals remain nonbonding (Scheme 1). The magnetic susceptibility measurement of **1** does show ferromagnetic interaction between Ni^{II} ions. Therefore, the two antibonding MOs having two spins must be energetically close enough to stabilize the high-spin state.

Acknowledgment. This work was supported in part by a Grant-in-aid for Scientific Research (No. 08640705) from the Ministry of Education, Science, and Culture.

Supporting Information Available: Tables S1−S4, listing detailed crystallographic data, atomic coordinates of hydrogen atoms, anisotropic temperature factors, and bond lengths and angles (4 pages). Ordering information is given on any current masthead page.

IC970180M